Rates of shortening, propagation, underthrusting, and flexural wave migration in continental orogenic systems

P.G. DeCelles Department of Geosciences, University of Arizona, Tucson, Arizona 85721, USA
P.C. DeCelles Trinity School at Greenlawn, South Bend, Indiana 46617, USA

ABSTRACT

The rate of horizontal shortening in an orogenic wedge is the rate at which the length of undeformed crust decreases as it is incorporated into the orogen. This rate equals the rate of convergence of the foreland lithosphere toward the central surface of the orogenic belt and the rate of subduction of foreland lithosphere beneath the central surface. The rate of propagation of an orogenic wedge is the rate at which it elongates in the direction of horizontal shortening. This rate is controlled by the rates of mass accretion to the orogenic wedge and erosion. The orogenic belt drives a flexural isostatic wave through the foreland lithosphere at a velocity equal to the rate of propagation plus the rate of subduction (or convergence or shortening). In orogenic belts where the total amount of shortening cannot be reliably estimated from balanced regional cross sections, it may be possible to determine total shortening from the distance of flexural wave migration in the foreland basin and the width of the orogenic wedge. In addition, orogenic wedges may accelerate solely in response to a reduction in taper.

Keywords: fold-and-thrust belts, Himalayas, Andes, rates.

INTRODUCTION

The rate of shortening is one of the fundamental properties of an orogenic belt, partly controlling its geometry, internal structure, grade of metamorphism, regional elevation, rates of surface and rock uplift, and the velocity of the flexural isostatic wave that is set up in the foreland lithosphere adjacent to the growing load of the fold-and-thrust belt. Thus there are many reasons for determining rates and amounts of shortening in fold-and-thrust belts. Unfortunately, acquiring and interpreting the data necessary to establish the rate of shortening constitute a daunting task. In addition, no clearly defined set of terms has been employed to describe the several different types of horizontal displacements that occur in fold-and-thrust belts and the relationships among them. Terms such as shortening, convergence, propagation, and thrusting are used interchangeably and inconsistently to describe different processes. The purposes of this paper are to (1) clarify the terminology for understanding the various rates in fold-and-thrust belts and (2) present a simple geometric formulation that illustrates the relationships among the various rates and allows for estimates of total orogenic shortening based on the large-scale geodynamics of the orogenic wedge and foreland-basin system.

DEFINITIONS

Figures 1 and 2 define the six rates of large-scale processes (subduction, convergence, underthrusting, shortening, propagation, and flexural wave migration) that operate in contractional orogenic belts. We consider only horizontal processes, rather than processes related to vertical motions (England and Molnar, 1990). Figure 1 schematically illustrates in transverse cross section a doubly tapered orogenic belt, growing in response to orthogonal convergence (with only in-plane strain) of an oceanic and a continental plate. The following derivations are for only one side of the system, but similar relationships can be derived for both sides and for orogenic belts developed between any two converging plates. The vertical orientation of the subducting slabs is shown for simplicity and ultimately has no effect on the derivations.

The central surface divides the orogen lengthwise into two oppositely verging wedges composed of rocks derived from the two plates. The logical choice for a central surface in a collisional orogen is the suture zone. In an oceanic-continental orogenic belt the axis of the magmatic arc may be a suitable choice. However, the arc is seldom stable over the entire history of an orogenic belt because of changes in oceanic subduction angle and tectonic erosion of the forearc region (e.g., Allmendinger et al., 1997). In addition, it is unlikely that the central surface is a simple vertical plane. Even in such cases, however, the boundary between the forearc and retroarc provinces can commonly be estimated within a few tens of kilometers. Bearing these caveats in mind, the rates of foreland and oceanic convergence (C_f and C_o, respectively) are defined as the rates at which points fixed to each plate move toward the central surface, and the total convergence (C_{total}) is their sum (Fig. 1). The converging plates are subducted at rates of V_{sf} and V_{so}, respectively.

As undeformed rocks are incorporated into the orogenic wedge, they are shortened at a rate S. The orogen grows by accretion of rock from the two plates, causing the tips of the oppositely verging orogenic wedges to propagate outward from the central surface. On the continental side, the tip of the retroarc orogenic wedge propagates at a rate P toward the craton. The foreland lithosphere underthrusts the fold-and-thrust belt at a rate U (Fig. 2). The orogenic load sets up a standing flexural wave in the subducting foreland lithosphere, which migrates through the lithosphere at a velocity F.

The relationships among S, V_{sf}, C_f, F, U, and P are illustrated in Figure 2. The foreland crust is divided into upper and lower parts. The upper crust delaminates and shortens as the lower crust is subducted. Assuming constant volumes and thicknesses of the converg-

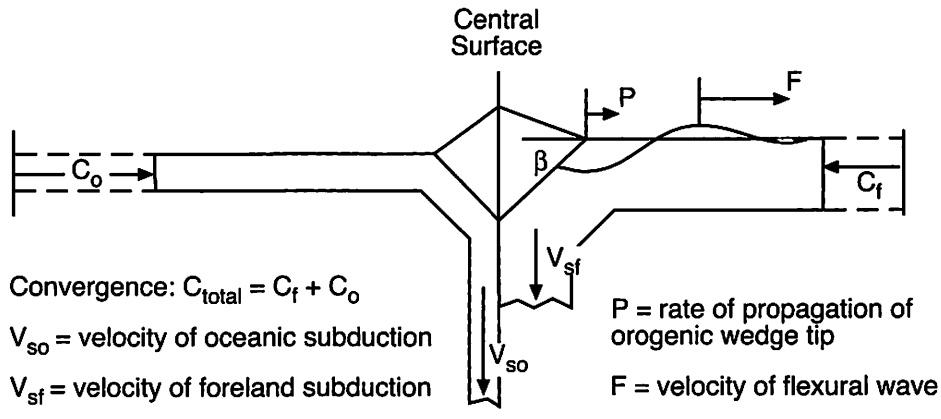

Figure 1. Schematic transverse cross section of oceanic-continental orogenic system, defining various rates discussed in text.

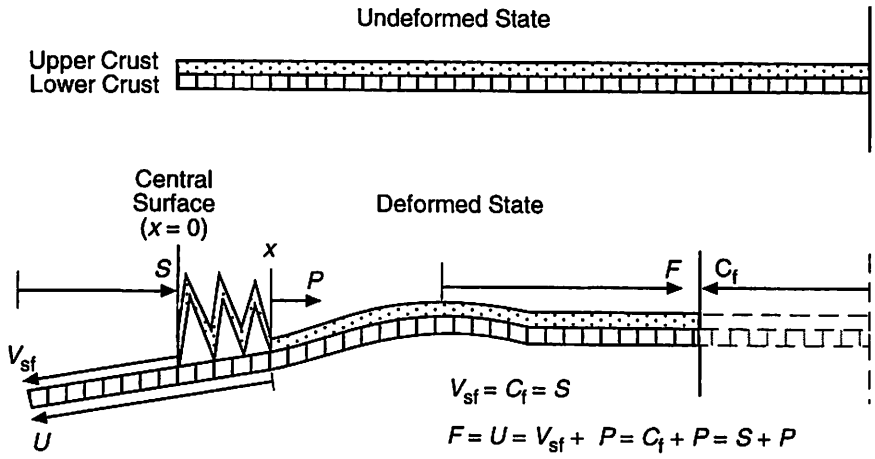

Figure 2. Simplified cross sections in undeformed (above) and deformed (below) states illustrating length budgets of upper crust and lower crust in contractional orogenic belt and relationships among parameters discussed in text.

ing plates, the rates of convergence, subduction, and shortening are equal. If the elastic properties of the foreland lithosphere do not change, the distance of flexural wave migration over time t is $F \cdot t$, which is equal to $S \cdot t + x$, where x is the length of the orogenic wedge in the transport direction. The total distance of underthrusting $U \cdot t$ is the sum of the subduction distance and the propagation distance.

VALUES OF F AND P AS A FUNCTION OF V_{sf}

The rates of propagation and flexural wave migration depend upon the rate of increase in the size of the orogenic wedge. The rate of propagation of the wedge tip is the rate of lengthening of the wedge, dx/dt. For a tapered orogenic wedge, the cross-sectional area of the lower triangular part of the wedge (dot pattern in Fig. 3) is

$$A = \frac{x^2 \tan \beta}{2}, \tag{1}$$

where β is the dip of the basal décollement. The time rate of change of this area is

$$\frac{dA}{dt} = \left(x \tan \beta \frac{dx}{dt}\right) + \left(\frac{x^2}{2 \cos^2 \beta} \cdot \frac{d\beta}{dt}\right). \tag{2}$$

Employing a small-angle approximation for β and solving equation 2 for dx/dt yields the rate of propagation (P) of the orogenic wedge as a function of changes in A and β:

$$\frac{dx}{dt} = P = \frac{1}{x\beta}\left(\frac{dA}{dt} - \frac{x^2}{2} \cdot \frac{d\beta}{dt}\right). \tag{3}$$

For orogenic wedges that maintain constant taper by self-similar growth (e.g., Davis et al., 1983), equation 3 reduces to

$$\frac{dx}{dt} = P = \frac{1}{x\beta} \cdot \frac{dA}{dt}. \tag{4}$$

However, β probably decreases systematically with time in many orogenic wedges, as the wedge incorporates progressively stronger, more structurally competent rocks while migrating toward the craton interior (Mitra, 1997). We assume that β decreases linearly from β_0 to β_f over the lifetime of the orogenic wedge according to $\beta(t) = K(t - t_f) + \beta_f$, where $K = (\beta_f - \beta_0)/(t_f - t_0)$ and t_f and t_0 are, respectively, the final and initial times of activity of the orogenic wedge. At any time during the lifetime of the orogenic wedge, t is simply its age. The rate of change in cross-sectional area (dA/dt) is the product of the rate of subduction, the thickness (T) of rock in the foreland plate that accretes to the orogenic wedge, and the fraction (E) of this rock that survives erosion to actually build the wedge:

$$\frac{dA}{dt} = V_{sf} TE. \tag{5}$$

For a wedge undergoing no erosion, $E = 1$. Substituting equation 5 into equation 3 and solving the differential equation yields

$$x = \left(\frac{\beta_0(|B| + x_0^2)}{|K|\left(\frac{\alpha}{|K|} - t\right)} - |B|\right)^{1/2}, \tag{6}$$

where $\alpha = \beta_f - Kt_f$ and $B = (2V_{sf}TE)/K$. We use absolute values because $\beta_f < \beta_0$. Equation 6 provides the relationship between the length of the wedge (x) and time (t), for a given change in β.

The derivative of x with respect to t provides the rate of propagation (P) of the wedge:

$$P = \frac{|K|}{2x\beta_0} \cdot \left[\frac{(|B| + x^2)^2}{|B| + x_0^2}\right]. \tag{7}$$

The rate of propagation must be added to the rate of shortening (which is equal to the rates of subduction and convergence) to yield the velocity of the flexural wave that migrates through the foreland lithosphere (Fig. 2). From equation 5 it follows that the area of the lower part of the wedge is equal to the rate at which rock is added to the wedge times the amount of time during which the wedge is active, or

$$\frac{x^2\beta}{2} = V_{sf} TE \cdot t + W, \tag{8}$$

where x is the length of the wedge at time t and W is a constant. In our model $W = 0$ because we assume that all of the mass of the wedge is due to thrusting. Equations 6 and 7 provide a view of the long-term evolution of the fold-and-thrust belt, and equation 8 and the relationship $F \cdot t = S \cdot t + x$ are useful rules of thumb that provide estimates of key thrust-belt parameters. Two important caveats must be kept in mind. First, it is likely that the flexural rigidity of the foreland lithosphere increases through time as older, colder lithosphere is underthrust beneath the orogenic wedge. This change would increase F through time, without corresponding changes in S and P. Thus the sum $S \cdot t + x$ provides only a minimum value of $F \cdot t$. Similarly, our model does not account for possible viscous relaxation of the flexural wave through time. Second, the model is limited to values of x tan $\beta_0 \geq ET$. For $x < ET/\tan \beta_0$, the wedge-building mechanism is more complicated. Therefore, P has a value V_{sf} at $x = x_0 = ET/\tan \beta_0$,

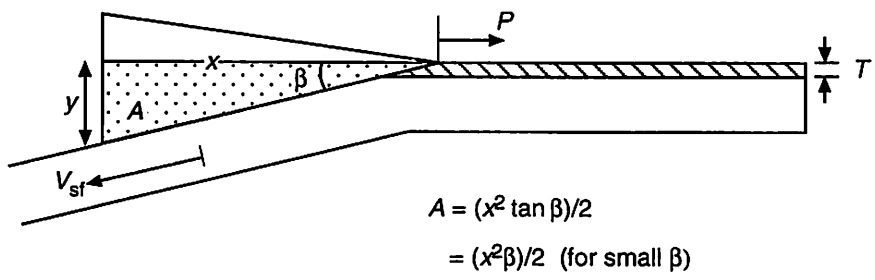

Figure 3. Schematic cross section of orogenic wedge with basal décollement slope of β, growing by accretion of material of thickness T from slab subducting at rate of V_{sf}.

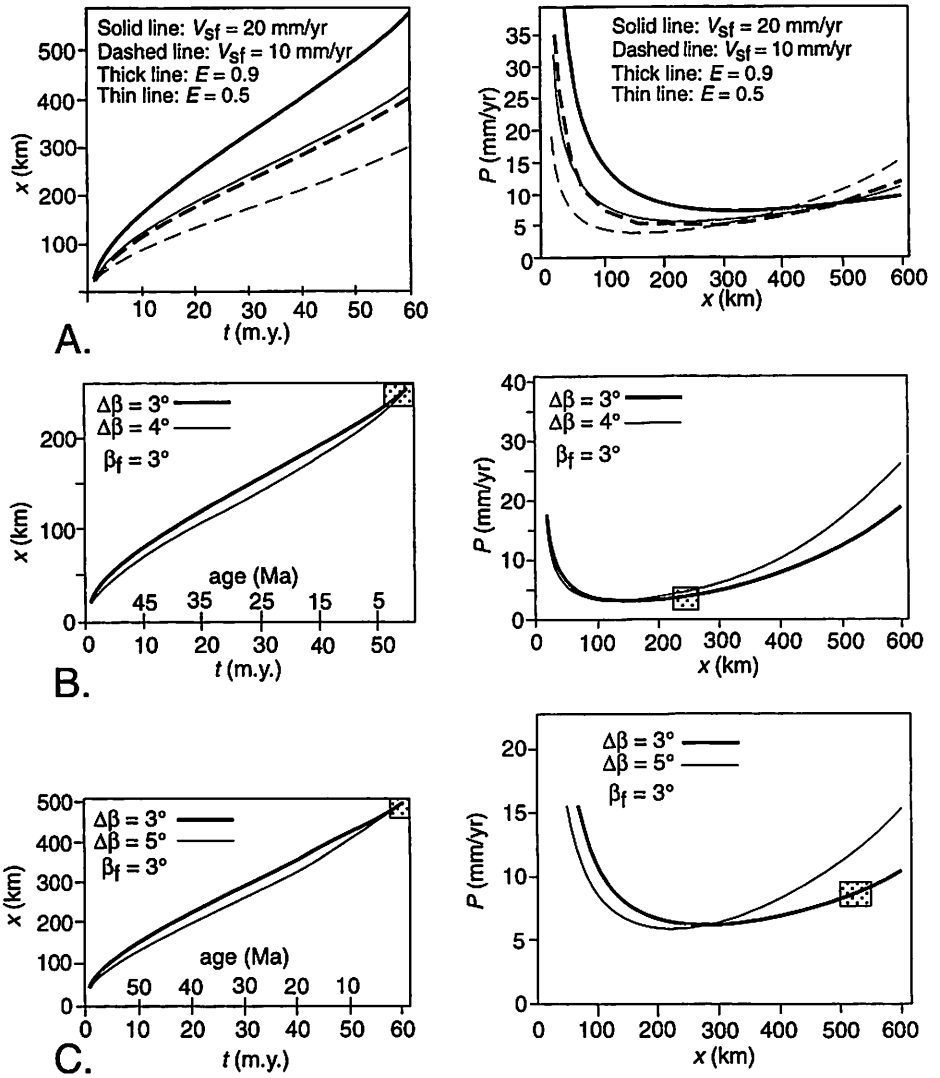

Figure 4. A: Length (x) vs. time (t) and propagation rate (P) vs. length plots for orogenic wedges with β_0 = 6° and β_f = 3°, illustrating effects of different subduction (or shortening) rates and erosion constant (E). B and C: Length vs. time and propagation rate vs. length curves for different values of erosion constant (E) and range of changes in basal décollement dip. B: Himalayan case, in which subduction rate is 17.5 mm/yr, T = 7 km, E = 0.25, and β_f = 3°. C: Andean case, in which subduction rate is 15 mm/yr, T = 8 km, E = 0.9, and β_f = 3°. Boxes with dot pattern represent present ranges of x, t, and P for fold-and-thrust belts in Nepal and southern Bolivia.

which is the lower limit of x for which the model can work.

APPLICATIONS

In general, the rate of propagation of an orogenic wedge can be expected to decrease through time as it enlarges because larger wedges require greater amounts of mass influx to continue to grow. For typical values of V_{sf}, T, and E, the decreasing rate of propagation is most pronounced during the first ~10 m.y. and ~100 km of growth in x (Fig. 4). Orogenic wedges with constant β continue to decelerate throughout their lifetime, but wedges in which β decreases through time undergo a decline in P until $x = x_{min} = (|B|/3)^{1/2}$, at which point the propagation rate begins to increase (Fig. 4). This acceleration takes place because the decreasing taper of the wedge reduces its ability to grow upward, so it must propagate (i.e., elongate) increasingly rapidly to accommodate the continuing influx of rock across the basal décollement.

The relationships in equation 8 and Figure 2 can be applied to orogenic belts where space geodetic data are available to provide rates of shortening and convergence. In the Nepalese Himalaya, V_{sf} of the Indian plate is 17.5 ± 2 mm/yr (Bilham et al., 1997). The basal décollement dips northward at ~3°–4° (Schelling, 1992; DeCelles et al., 1998a). The average thickness of recently accreted thrust sheets in the Lesser Himalaya and Subhimalaya is ~7 km. The present length of the fold-and-thrust belt in the transport direction (x_f) is ~250 km. The age of the fold-and-thrust belt in Nepal is ca. 55 Ma. Solving equation 8 for E using these values for the other parameters yields $E \cong 0.24$–0.32. This implies that less than a third of the mass going into the orogenic wedge survives erosion to build topography. The predicted rate of propagation of the fold-and-thrust belt is ~3 mm/yr (Fig. 4B), which must be added to the rate of Indian plate subduction to produce a total rate of underthrusting of ~20.5 mm/yr. For comparison, Bilham et al. (1997) calculated the present rate of underthrusting of Indian lithosphere beneath the Nepalese Himalaya to be 20.5 ± 2 mm/yr.

A similar analysis of the arid central Andean orogenic wedge in southern Bolivia using V_{sf} = 15 mm/yr (Norabuena et al., 1998), x_f = 500 km, β_f = 3°, T = 8 km (Dunn et al., 1995), and t_f = 60 m.y. yields $E \cong 0.91$. In contrast to the rapidly eroding Himalaya, almost all of the mass that has gone into the Andean orogenic wedge at the latitude of southern Bolivia has survived erosion to build the wedge (Fig. 4C), presumably because of the arid climate, which limits erosion (Masek et al., 1994; Allmendinger et al., 1997; Horton, 1999).

The rates determined by the geodetic studies are based on observations over only a few years and may not be representative of the long-term history of the Himalayan and Andean fold-and-thrust belts. If values of V_{sf}, T, E, and β can be estimated back through time, equations 6 and 7 can be used to reconstruct the propagation history of the orogenic wedge. On the basis of seafloor magnetic anomalies and shortening rates in Asia, total shortening in the Himalaya should be ~900–1000 km (Le Pichon et al., 1992, and references therein). The long-term average rate of shortening is thus ~16–18 mm/yr, approximately equal to the present rate (Bilham et al., 1997). Restorations of regional balanced cross sections in Nepal and India suggest similar rates of shortening throughout Neogene time (DeCelles et al., 1998a; Powers et al., 1998). Estimates of Paleogene shortening rates are not available. In Figure 4B, we plot the length versus time and propagation versus length histories of the Himalayan orogenic wedge, using the parameter values discussed here. The plot predicts that P decreased rapidly during the first 15 m.y. of shortening in the Himalaya. Since ca. 35 Ma, P has been ~3–4 mm/yr, but the curves suggest that since the thrust belt reached a length of ~112–145 km (depending on the actual change in β), corresponding to ages between ca. 35 Ma and 25 Ma, the propagation rate has been accelerating. Combining these changing values of P with the approximately constant value of S suggests that the velocity of the flexural wave in the Himalayan foreland basin has generally decreased from Paleogene to Neogene time, as suggested by the foreland stratigraphic record (DeCelles et

al., 1998b). The total distance of southward migration of the flexural wave is predicted to be 250 km + 950 km = 1200 km (Fig. 2), which over the 55 m.y. lifetime of the orogen has taken place at a long-term average rate of ~22 mm/yr.

Figure 4C shows a similar analysis of the Andean orogenic wedge at the latitude of central Bolivia. Total shortening in the Andes is not currently known, so we project the present value of V_{sf} (~15 mm/yr, Norabuena et al., 1998) back through time. The P versus x curve (Fig. 4C) suggests that the Andean orogenic wedge has also accelerated and should be propagating at a present rate of ~8–12 mm/yr. A long-term average propagation rate of ~8 mm/yr can be estimated by dividing the present width of the wedge in Bolivia (~500 km) by the amount of time since the onset of shortening (~60 m.y.).

The relationship $F \cdot t = S \cdot t + x$ provides a means of estimating the total shortening in an orogenic wedge if estimates of the total distances of propagation and migration of the flexural wave can be determined. The migration history of the flexural wave can be assessed from the migration history of the foreland basin (Lyon-Caen and Molnar, 1985; Sinclair, 1997; DeCelles et al., 1998b). For example, the rate of migration of the North Alpine foreland basin during Eocene-Miocene time was ~8.5–12.9 mm/yr (Sinclair, 1997). The average rate of propagation of the North Alpine orogenic wedge is simply its present length divided by the amount of time that passed during its growth, or ~2.6 mm/yr (~100 km/38 m.y.; Pfiffner, 1986; Sinclair, 1997). This result suggests that the rate of shortening was ~5.9–10.3 mm/yr. The rate determined from restoration of balanced cross sections is 7–10 mm/yr (Pfiffner, 1986).

DISCUSSION

This analysis, crude as it is, yields interesting results. First, although changes in erosion and subduction rates can have a dramatic effect on the geometry and propagation rate of an orogenic wedge, equation 7 suggests that long-term accelerations in propagation velocity are to be expected in fold-and-thrust belts that undergo long-term reductions in taper (Fig. 4). These accelerations do not require changes in external factors such as convergence or erosion rates.

Second, it may be possible to estimate shortening (and shortening rate) by making some simple geometric observations in orogenic wedges. Shortening rates in fold-and-thrust belts are usually determined by dividing the shortening distance of balanced cross sections by the amount of time that elapsed during shortening. Long-term average rates determined by this method are in the range of 2–20 mm/yr, or ~10%–40% of the rates of associated plate convergence. The cross-sectional approach to estimating shortening relies on assumptions implicit in the construction of balanced cross sections (Boyer and Elliott, 1982; Woodward et al., 1988), which are normally valid only in the frontal, unmetamorphosed part of the orogenic wedge. Even in the frontal orogenic wedge, microstrain may produce significant cryptic shortening that is seldom incorporated into balanced restorations (Mitra, 1997). In the hinterland, deformation is commonly ductile, hanging-wall cutoffs are eroded, and Barrovian metamorphism may involve significant volume changes. Thus, attempts to determine total shortening across major orogens by using balanced cross sections often fall short of explaining the total shortening required by other indicators, such as total crustal thickness (Kley and Monaldi, 1998) or plate tectonic reconstructions (Le Pichon et al., 1992). The use of the flexural wave migration distance as an estimate of total propagation plus shortening distance overcomes the difficulties of directly measuring shortening across an entire orogenic belt.

ACKNOWLEDGMENTS

Supported by National Science Foundation grant EAR-9804680. We are grateful to Karl Mueller and Gene Humphreys for helpful reviews.

REFERENCES CITED

Allmendinger, R.W., Jordan, T.E., Kay, S.M., and Isacks, B.L., 1997, The evolution of the Altiplano-Puna Plateau of the central Andes: Annual Review of Earth and Planetary Sciences, v. 25, p. 139–174.

Bilham, R., Larson, K., and Freymuller, J., 1997, Indo-Asian convergence rates in the Nepal Himalaya: Nature, v. 386, p. 61–64.

Boyer, S.E., and Elliott, D., 1982, Thrust systems: American Association of Petroleum Geologists Bulletin, v. 66, p. 1196–1230.

Davis, D., Suppe, J., and Dahlen, F.A., 1983, Mechanics of fold-and-thrust belts and accretionary wedges: Journal of Geophysical Research, v. 88, p. 1153–1172.

DeCelles, P.G., Gehrels, G.E., Quade, J., Kapp, P.A., Ojha, T.P., and Upreti, B.N., 1998a, Neogene foreland basin deposits, erosional unroofing, and the kinematic history of the Himalayan fold-and-thrust belt, western Nepal: Geological Society of America Bulletin, v. 110, p. 2–21.

DeCelles, P.G., Gehrels, G.E., Quade, J., and Ojha, T.P., 1998b, Eocene–early Miocene foreland basin development and the history of Himalayan thrusting, western and central Nepal: Tectonics, v. 17, p. 741–765.

Dunn, J.F., Hartshorn, K.G., and Hartshorn, P.W., 1995, Structural styles and hydrocarbon potential of the sub-Andean thrust belt of southern Bolivia, *in* Tankard, A.J., et al., eds., Petroleum basins of South America: American Association of Petroleum Geologists Memoir 62, p. 523–543.

England, P., and Molnar, P., 1990, Surface uplift, uplift of rocks and exhumation of rocks: Geology, v. 18, p. 1173–1177.

Horton, B.K., 1999, Erosional control on the geometry and kinematics of thrust belt development in the central Andes: Tectonics, v. 18, p. 1292–1304.

Kley, J., and Monaldi, C.R., 1998, Tectonic shortening and crustal thickness in the Central Andes: How good is the correlation?: Geology, v. 26, p. 723–726.

Le Pichon, X., Fournier, M., and Jolivet, L., 1992, Kinematics, topography, shortening, and extrusion in the India-Eurasia collision: Tectonics, v. 11, p. 1085–1098.

Lyon-Caen, H., and Molnar, P., 1985, Gravity anomalies, flexure of the Indian plate, and the structure, support and evolution of the Himalaya and Ganga Basin: Tectonics, v. 4, p. 513–538.

Masek, J.G., Isacks, B.L., Gubbels, T.L., and Fielding, E.J., 1994, Erosion and tectonics at the margins of continental plateaus: Journal of Geophysical Research, v. 99, p. 13,941–13,946.

Mitra, G., 1997, Evolution of salients in a fold-and-thrust belt: The effects of sedimentary basin geometry, strain distribution and critical taper, *in* Sengupta, S., ed., Evolution of geological structures in micro- to macro-scales: London, Chapman & Hall, p. 59–90.

Norabuena, E., Leffler-Griffin, L., Mao, A., Dixon, T., Stein, S., Sacks, I.S., Ocola, L., and Ellis, M., 1998, Space geodetic observations of Nazca–South America convergence across the central Andes: Science, v. 279, p. 358–362.

Pfiffner, O.A., 1986, Evolution of the north Alpine foreland basin in the Central Alps, *in* Allen, P.A., and Homewood, P., eds., Foreland basins: International Association of Sedimentologists Special Publication 8, p. 219–228.

Powers, P.M., Lillie, R.J., and Yeates, R.S., 1998, Structure and shortening of the Kangra and Dehra Dun reentrants, sub-Himalaya, India: Geological Society of America Bulletin, v. 110, p. 1010–1027.

Schelling, D., 1992, The tectonostratigraphy and structure of the eastern Nepal Himalaya: Tectonics, v. 11, p. 925–943.

Sinclair, H.D., 1997, Tectonostratigraphic model for underfilled peripheral foreland basins: An Alpine perspective: Geological Society of America Bulletin, v. 109, p. 324–346.

Woodward, N.B., Boyer, S.E., and Suppe, J., 1988, Balanced geological cross sections: An essential technique in geologic research and exploration: 28th International Geological Congress Short Course in Geology 6: Washington, D.C., American Geophysical Union, 132 p.

Manuscript received April 21, 2000
Revised manuscript received October 19, 2000
Manuscript accepted November 5, 2000

Printed in USA